JBC Papers in Press. Published on June 22, 2004 as Manuscript M405217200

Novel Protein-Protein Interactions of the *Yersinia pestis* Type III Secretion System Elucidated With a Matrix Analysis by Surface Plasmon Resonance and Mass Spectrometry

Wieslaw Swietnicki[*], Sarah O'Brien[*], Kari Holman[*], Ernst Brueggeman[*], Joseph E. Tropea[†], Harry Hines[*], David S. Waugh[†], and Robert G. Ulrich[*]

[*]U.S. Army Medical Research Institute of Infectious Diseases, and [†]Macromolecular Crystallography Laboratory, National Cancer Institute at Frederick, Frederick, MD 21702

Running title: Interactions of Type III Secretion System

Abbreviations footnote: MALDI-TOF – matrix-assisted laser desorption – time-of-flight mass spectrometry, MS – mass spectrometry, PBS – phosphate-buffered saline, RU – refractive unit, SPR – surface plasmon resonance, TTSS – type three secretion system, YopH/N – N-terminal (amino acids 1-129) part of YopH, YopH/C – C-terminal (amino acids 164 - 468) part of YopH, *Y. enterocolica* – *Yersinia enterocolica*, *Y. pestis* – *Yersinia pestis*.

Report Documentation Page

Form Approved
OMB No. 0704-0188

Public reporting burden for the collection of information is estimated to average 1 hour per response, including the time for reviewing instructions, searching existing data sources, gathering and maintaining the data needed, and completing and reviewing the collection of information. Send comments regarding this burden estimate or any other aspect of this collection of information, including suggestions for reducing this burden, to Washington Headquarters Services, Directorate for Information Operations and Reports, 1215 Jefferson Davis Highway, Suite 1204, Arlington VA 22202-4302. Respondents should be aware that notwithstanding any other provision of law, no person shall be subject to a penalty for failing to comply with a collection of information if it does not display a currently valid OMB control number.

1. REPORT DATE	2. REPORT TYPE	3. DATES COVERED
10 SEP 2004	**N/A**	**-**

4. TITLE AND SUBTITLE	5a. CONTRACT NUMBER
Novel protein-protein interactions of the Yersinia pestis type III secretion system elucidated with a matrix analysis by surface plasmon resonance and mass spectrometry, Journal of Biological Chemistry 279:38693 - 38700	5b. GRANT NUMBER
	5c. PROGRAM ELEMENT NUMBER
6. AUTHOR(S)	5d. PROJECT NUMBER
Swietnicki, W O'Brien, S Holman, K Brueggemann, E Tropea, J Hines, H Waugh, DS Ulrich, RG	5e. TASK NUMBER
	5f. WORK UNIT NUMBER
7. PERFORMING ORGANIZATION NAME(S) AND ADDRESS(ES)	8. PERFORMING ORGANIZATION REPORT NUMBER
United States Army Medical Research Institute of Infectious Diseases, Fort Detrick, MD	**RPP-03-33**
9. SPONSORING/MONITORING AGENCY NAME(S) AND ADDRESS(ES)	10. SPONSOR/MONITOR'S ACRONYM(S)
	11. SPONSOR/MONITOR'S REPORT NUMBER(S)

12. DISTRIBUTION/AVAILABILITY STATEMENT

Approved for public release, distribution unlimited

13. SUPPLEMENTARY NOTES

The original document contains color images.

14. ABSTRACT

Binary complexes formed by components of the Yersinia pestis type III secretion system were investigated by surface-plasmon resonance (SPR) and matrix-assisted laser desorption time-of-flight (MALDI-TOF) mass spectrometry. Pair-wise interactions between fifteen recombinant Yersinia outer proteins (Yops), regulators and chaperones were first identified by SPR. Mass spectrometry confirmed over 80% of the protein-protein interactions suggested by SPR, and new binding partners were further characterized. The Yop secretion protein (Ysc) M2 of Y. enterocolitica and LcrQ of Y. pestis, formerly described as ligands only for the specific Yop chaperone (Syc) H, formed stable complexes with SycE. Additional previously unreported complexes of YscE with the translocation-regulator protein TyeA and the thermal-regulator protein YmoA, and multiple potential protein contacts by YscE, YopK, YopH, and LcrH were also identified. Because only stably folded proteins were examined, the interactions we identified are likely to occur either before or after transfer through the injectosome to mammalian host cells, and may have relevance to understanding disease processes initiated by the plague bacterium.

15. SUBJECT TERMS

Yersinia pestis, plague, protein assembly, surface plasmon resonance, type III secretion

16. SECURITY CLASSIFICATION OF:			17. LIMITATION OF ABSTRACT	18. NUMBER OF PAGES	19a. NAME OF RESPONSIBLE PERSON
a. REPORT	b. ABSTRACT	c. THIS PAGE			
unclassified	**unclassified**	**unclassified**	**SAR**	**8**	

Abstract

Binary complexes formed by components of the *Yersinia pestis* type III secretion system were investigated by surface-plasmon resonance (SPR) and matrix-assisted laser desorption – time-of-flight (MALDI-TOF) mass spectrometry. Pair-wise interactions between fifteen recombinant Yersinia outer proteins (Yops), regulators and chaperones were first identified by SPR. Mass spectrometry confirmed over 80% of the protein-protein interactions suggested by SPR, and new binding partners were further characterized. The Yop secretion protein (Ysc) M2 of *Y. enterocolitica* and LcrQ of *Y. pestis*, formerly described as ligands only for the specific Yop chaperone (Syc) H, formed stable complexes with SycE. Additional previously unreported complexes of YscE with the translocation-regulator protein TyeA and the thermal-regulator protein YmoA, and multiple potential protein contacts by YscE, YopK, YopH, and LcrH were also identified. Because only stably folded proteins were examined, the interactions we identified are likely to occur either before or after transfer through the injectosome to mammalian host cells, and may have relevance to understanding disease processes initiated by the plague bacterium.

Introduction

The plague bacillus *Yersinia pestis* and many other gram-negative pathogenic bacteria use a cell contact-dependent, type III secretion system (TTSS) for the highly-regulated transport of virulence factors across the bacterial cell envelope and into host cells. *Yersinia* outer proteins (Yops) are virulence factors encoded by a 70 kb plasmid (pCD1) of *Y. pestis*. An estimated 44 of the 96 potential open reading frames on pCD1 encode proteins that are directly involved in the assembly and regulation of the TTSS (Table I). There are 29 Yop secretion (Ysc) proteins, and within this group 10 have homologs in the bacterial flagellum (1). A larger number are conserved in other type III secretion systems. The Ysc proteins assemble into the injectosome, a macromolecular delivery system that directs the vector translocation of at least six effector Yops (YopE, YopH, YopJ, YopM, YopT, and YpkA) from the bacterium directly into the cytosol of mammalian cells (reviewed in ref. 2).

YopB and YopD, in conjunction with LcrV, are thought to form a pore in the membrane of mammalian cells through which the Yops (3, 4) are delivered. The cellular targets of some Yops are known. For example, YopH is a potent tyrosine phosphatase that dephosphorylates macrophage p130Cas and FAK proteins and disrupts focal adhesions (5-7), YopE is a GTPase-activating protein that causes actin cytoskeleton depolymerization (8), and YpkA is a Ser/Thr kinase that interferes with Rho-mediated cellular signaling (9). Recent data suggest that YopM targets the cellular kinases protein kinase C-like 2 and ribosomal S6 protein kinase 1 (10). Transport of YopB, YopD, YopE, YopH, and YopT

through the injectosome (11-13) is facilitated by formation of a complex between the secreted protein and a specific Yop chaperone (Syc), also encoded by pCD1. The three other effectors, YopJ, YopM, and YopO (YpkA), do not appear to require cognate secretion chaperones for transport (13). Comparatively little is known about the transient interactions involved in the assembly of the injectosome, the precise order of assembly, and delivery of the bacterial proteins into mammalian cells, and the energy source for the transport. To add to the complexity of the problem, protein-RNA and protein-DNA interactions are postulated for some components of the TTSS (14, 15). Deleting any single component of the TTSS attenuates bacterial virulence, suggesting that the Yops, Sycs, and other accessory proteins assemble into a large multi-subunit complex. As an essential component of the coordinately regulated low-Ca^{++} response stimulon (LCR) of pCD1, LcrF stimulates maximum expression of LcrV and Yops at 37ºC, and this activation step requires host cell contact or Ca^{++} depletion (16, 17).

As an approach to study the assembly of the *Y. pestis* virulence machinery, we used a two-step screening process to identify direct interactions between pairs of TTSS proteins. Protein interactions were first detected by surface plasmon resonance (SPR) and then classified according to the strength of interaction at equilibrium. Positive interactions indicated by SPR were next confirmed by MALDI-TOF mass spectrometry. Our results suggest that the combination of SPR and MALDI-TOF mass spectrometry is a powerful method for rapidly identifying protein-protein interactions involved in complex macromolecular assemblies such as the type III secretion system.

Materials and Methods

Protein expression and purification. The open reading frames (ORFs) encoding *Y. pestis* YopK, LcrG, LcrH, LcrQ, and YmoA were amplified from genomic DNA from *Y. pestis* biovar Orientalis, strain 195/P, kindly provided by Pat Worsham (USAMRIID), by polymerase chain reaction (PCR), using gene-specific primers with unpaired 5' extensions that added a TEV protease recognition site and a hexahistidine tag (6xHis-tag) to the N- and C-termini of each ORF, respectively. Because the *Y. pestis* and *Y. pseudotuberculosis* protein LcrQ is identical in amino acid sequence to YscM1 of *Y. enterocolitica*, both proteins will be referred to as YscM1 to avoid confusion. These amplicons were subsequently used as the template for a second PCR with primers PE-277 and PE-278 (18), which are designed to anneal to the TEV site and His-tag, respectively, and add attB recombination sites to the ends of the amplicon. The final PCR amplicon was inserted by recombinational cloning first into pDONR201 (Invitrogen, Inc.) and then into the MBP fusion vector pKM596 as described (19). Expression vectors for the production of *Y. pestis* YopR, TyeA, YscP, and YscE were constructed in a similar fashion, except that the 6xHis-tag was positioned between the TEV protease recognition site and the N-terminus of the *Y. pestis* protein instead of at its C-terminus. The same strategy was used to produce YopM and YscM2, using genomic DNA from *Y. enterocolitica* (strain WA, serotype 0:8), kindly provided by Susan Straley (Univ. of Kentucky). A polypeptide comprising residues 1-138 of *Y. pestis* SycH was co-expressed in *E. coli* with residues 29-78 of *Y. pestis* YscM1 fused to the C-terminus of MBP. A substantial amount of free (uncomplexed) SycH and YscM1 was isolated as byproducts of the procedure used to purify the

SycH/YscM1 complex. The untagged, C-terminal catalytic domain of YopH (D356A mutant) was expressed from a T7 promoter vector as described (19). Untagged *Y. pestis* SycE, N-terminal domain of *Y. pestis* YopH (residues 1-130) and F1 (residues 1-170) were produced as described previously (18, 20, 21). All recombinant *Yersinia* proteins were produced in *E. coli* BL21(DE3) cells and purified to homogeneity (determined by SDS gel electrophoresis) by a combination of affinity methods (amylose affinity chromatography and/or immobilized metal affinity chromatography) and conventional (size exclusion, ion exchange) chromatographic techniques. For some preparations, affinity columns were used to remove proteins containing affinity tags after enzymatic cleavage to yield native polypeptides. The molecular weights of the final products were confirmed by electrospray mass spectrometry.

Surface plasmon resonance. All measurements were performed on a Biacore 3000 instrument (Biacore Inc., Piscataway, NJ). Protein immobilization, binding experiments, and data analysis were performed with preexisting templates supplied with the instrument's software. In a typical experiment, 2000-3000 RU/flow cell of protein was immobilized on a CM5 chip using the amine coupling method. For binding experiments, each protein analyte in 10 mM potassium phosphate, pH 7.0, 150 mM NaCl, was passed over a chip surface at the flow rate of 20 μL/min for 3 min at 37^{o}C. The dissociation was followed for about 2 min in the same buffer and the surface was regenerated with 10 mM EDTA, pH 8.0, and 2 M NaCl. The cycle was repeated for every protein in the set. The chip surface was reused for up to 50 binding experiments. Data models were fitted using

Biacore software and exported to the Kaleidagraph program (Synergy Software, Inc.) for plotting.

All kinetic measurements were made at 20°C to extend the performance of the derivatized biosensor surfaces. In a typical experiment, 200-900 RU of protein was immobilized in a flow cell of a CM5 chip using a standard amine-coupling method. A test of concentration ranges and flow rates were used to optimize binding conditions, and duplicates of each analyte concentration were performed for kinetic analyses. Data were fitted to a Langmuir binding model, assuming stoichiometric (1:1) interactions and exported to Origin (Microcal Software, Inc.) for graphical presentation.

Mass spectrometry. In a typical experiment, proteins and buffer were mixed together to give a total of 20 μL of sample volume with final concentration of 5 μM of each protein in 10 mM potassium phosphate, pH 7.0, 150 mM NaCl. The solution was incubated at 37^{o}C for 30 min, and then a 5 μL aliquot was added to 3 μL of matrix (10 mg/mL of sinapinic acid in 50% acetonitrile, 0.02% trifluoroacetic acid, v/v) to give a 1.67:1 protein to matrix ratio (v/v). For mass spectra analysis, 1 μL of the protein-matrix solution was placed on a stainless steel sample grid and the spectra were acquired in delayed extraction mode using an externally calibrated Applied Biosystems Voyager-DE mass spectrometer (Framingham, MA) with the following operating conditions: an accelerating voltage of 25kV, a grid voltage of 93.2%, and a guide wire voltage of 0.3%. The scanned mass range was m/z 2,000 to approximately m/z 380,000, and 128 scans were averaged to yield each spectrum. The lowest possible laser power was used to generate spectra to prevent artificial peak formation.

Results

The TTSS polypeptides were expressed as full-length proteins or structural domains that were either native or His-tagged to facilitate purification (Table I). Criteria for inclusion of products in this study were that the proteins were required to be highly purified and stable in solution. Therefore, a final 15 of the potential 44 TTSS proteins were studied. Average surface densities of 3000 RU and analyte concentrations of 0.5-5 μM for each protein were used in SPR studies to favor higher affinity interactions. Preliminary studies performed at various pH values confirmed that the 6xHis tag present on some recombinant TTSS proteins did not directly influence protein binding. A matrix analysis (16 x 16) was performed, allowing each protein to be examined both covalently immobilized on the biosensor surface and also as an analyte free in solution. Each SPR measurement provided information about the relative strength and kinetics of interactions. Due to a high propensity of some TTSS proteins to form homodimers, the stoichiometry of binding interactions was ignored. Data below 50 response units (RU) were considered background, 50-100 RU weak, 100-300 RU medium, and above 300 RU as strong interactions. Although most of the recombinant proteins were similar in molecular mass, this classification was reassessed for smaller or larger proteins. A summary of all interactions is presented in Figure 1. From a potential 256 SPR interactions examined, 227 (88%) were nonproductive, 12 (5%) were weak, 9 (4%) medium, and 8 (3%) strong. Due to the amine-coupling method used to immobilize proteins to the chip surface, the

orientation influenced the interactions between some pairs of proteins. For example, when SycH was immobilized, binding to the YopH amino-terminal domain (YopH/N) was weak. Conversely, when YopH/N was immobilized, the interaction with SycH was stronger.

To confirm the interactions initially identified by SPR, we next examined complex formation by MALDI-TOF mass spectrometry. Representative mass spectra and a summary of the data are presented in Fig. 1 and Table II, respectively. The majority of the protein interactions detected by SPR (22 of 26) were confirmed by mass spectrometry (Fig. 1). For example, the high-affinity interactions between YscM2-SycH and YopH/N-SycH also produced strong mass/charge signals (Fig 3A and 3B). The interaction between TyeA and YopK, although weak by SPR, was still sufficient to detect complex formation by MALDI-TOF (Fig. 3C). In contrast, the weak interaction between YmoA and SycH detected by SPR was not be confirmed by MALDI-TOF. Similarly, the weak interactions between LcrG and F1 or YopK, identified by SPR, were not observed by mass spectrometry. The SPR results for YopH/N-TyeA interactions using a high ligand density surface were initially ambiguous. Upon re-evaluation with lower-density surfaces we could not observe YopH/N-TyeA complex formation, nor was complex observed in solution (see below). However, a YopH/N-TyeA species was detected by MALDI-TOF, hence the assignment of "weak" interactions for this particular complex. While data from MALDI-TOF and SPR were complimentary, a comparison of results also allowed us to eliminate some tentative complex assignments.

To investigate the potential protein-protein interactions in more detail, we performed a detailed kinetic analysis of select binding pairs by SPR (Fig. 2, Table III). In

addition, we also examined stable complex formation at equilibrium by mixing both components free in solution and isolating fractions by size-exclusion chromatography (SEC; Table III). The measured K_ds varied from low micromolar (YopH/N-SycH) to nanomolar range (SycH-YscM1). Binding affinities for SycH to ligands were: YscM1 > YscM2 ≥ YopH/N. In addition, all of the SycH complexes were stable in solution (Table III). The association rate for YscM1 was the fastest of the three SycH binding partners, but dissociation rates were almost identical. In contrast, YopH/N and YscM2 have very similar k_{on} and k_{off} rates for interaction with SycH, suggesting that the preferred binding partner for SycH is YscM1. The SycE/YscM1 and SycE/YscM2 were not previously reported, and these complexes were stable (Table III) when subjected to size exclusion chromatography (SEC). The YscM2-SycE complex has a relatively slow k_{off} rate (Table III) favoring stability in solution, as detected by SEC. Despite very fast k_{on} and k_{off} rates, YscM1-SycE complexes were also detected by SEC, whereas, the fast k_{on} and k_{off} rates, and consequential low affinity (K_d >5 μM, Table III), of TyeA-YscE interactions (Fig. 2 and Table III), did not favor complex formation with both partners in solution (SEC results). In addition, the sharp rise and drop of the signal in the binding and dissociation phases, respectively, of the YscM2-SycE sensogram (Fig. 2B), indicated fast k_{on} and k_{off} rates. The association rate for the SycH-YopH/N chaperone-ligand pair (Fig. 2B) was relatively fast but dissociation was slow, indicating a more stable interaction under the conditions examined. Finally, the weak YopK-TyeA interactions (Fig. 2C), exhibiting fast k_{on} and k_{off} rates, were not previously described.

Discussion

Few direct measurements are available for interactions between individual components of the TTSS, an essential virulence apparatus for several pathogenic bacterial species. Therefore, the results reported here may provide additional insight into the molecular mechanisms of bacterial virulence. We used recombinant TTSS proteins to identify new binding partners using two independent biophysical methods, and provide additional data for previously observed protein-protein interactions. Not all TTSS components could be examined because many are presently difficult to produce as stable recombinant proteins. In addition, secondary and 3-dimensional structures for most of these proteins are unknown. The membrane-spanning portion of the injectosome is hypothesized to serve as a conduit for the translocation of several proteins. For the previously reported SptP effector protein of *Salmonella* (22), binding to the SicP chaperone occurs in a partially unfolded state. Together with the fact that the narrow diameter of the external injectosome seems incompatible with the passage of folded, globular proteins, suggest that effector proteins may be secreted before acquiring their native conformations. Alternatively, secretion may favor partially unfolded proteins present in equilibrium with folded species. In any case, if unfolding is prerequisite for type III secretion, then the potential interactions we identified are likely to occur either before or after this stage in the process. As only stably folded proteins were used in our

study, the potential contribution of very hydrophobic or disordered polypeptides to binding interactions could not be addressed.

The observed stoichiometry for all protein complexes we detected by MALDI-TOF mass spectrometry was 1:1 (Table II), with the exception of a mixture of 1:1 and 2:1 for SycH-YscM2. Yet, the secretion chaperones are presumed to exist as homodimers in solution. For example, a crystal structure of the SycE-YopE complex (13) revealed that a dimer of SycE (residues 1-122) binds to one YopE truncated to residues 17-85 (2:1 stoichiometry). We also detected a 2:1 complex of SycE:YopE (data not shown) by MALDI-TOF mass spectrometry and amino acid analysis, using YopE truncated to residues 15-85 and co-expressed with SycE (residues 1-122). In contrast, a 1:1 complex was also observed by MALDI-TOF mass spectrometry of SycE and the amino-terminus of YopE (residues 1-90), co-expressed in E. coli (data not shown), suggesting that protein length contributes to the final complex formed. Hence, the significance of the stoichiometry observed in the MALDI-TOF mass spectrometry experiments is uncertain. Nevertheless, we are confident that the results are qualitatively valid for two reasons. First, we detected complexes between all pairs of proteins that were previously shown by other means to interact with each other (YopH/H-SycH, YscM1-SycH, YscM2-SycH, and SycE-YopE). Second, several pairs of apparently non-interacting proteins, as determined by SPR, were also analyzed by MALDI-TOF mass spectrometry (SycH-YscP, SycH-YopR, SycE-YscP, and SycE-YopR), and in no case were any complexes detected (data not shown).

Most previously reported binary complexes of TTSS components were identified by inference, using genetic deletions for example, and hence very little quantitative data

are available for these interactions. It is less likely that many of the protein-protein interactions identified in our study could be identified by biological screening alone, and the biological significance of these observed contacts has yet to be investigated. However, an examination of previous reports concerning the regulatory role of certain TTSS components suggests that our results may contribute to understanding some key steps in the assembly and function of the macromolecular secretion complex. Closure or disassembly of the contact-dependent secretion channel turns Yop synthesis off. The regulatory protein YscM1 is linked indirectly to controlling Yop expression and is produced by all pathogenic Yersiniae. Whereas YscM2 is expressed only by *Y. enterocolitica* and remains associated with the bacteria, it shares 59 % sequence identity with YscM1 and is believed to be functionally equivalent (23). In addition, SycH is required for secretion of YopH, YscM1 and YscM2 by *Y. enterocolitica* (23). Prior to contact with mammalian host cells, SycH was proposed (24) to interact with YscM1 in a hypothetical secretion substrate acceptor site, leading to down-regulation of Yop expression, while cell contact stimulates secretion of YscM1 and resumption of Yop expression. Although it is possible that YopH binding is influenced by the truncated catalytic domain, our data suggests that SycH -YscM1 interactions are favored kinetically over the slower forming and less stable SycH-YopH complex. In addition, the propensity to form a complex with SycH was retained by the N-terminal domain of YscM1. It is conceivable that secretion of YscM1 allows YopH association with SycH, although ligand exchange may require involvement of an additional factor or perhaps a conformational change. Unlike YopH, YopE is unstable unless bound to the cognate chaperone SycE. Therefore, we could not compare our results with YopH and SycH interactions directly

with the analogous YopE-SycE protein-chaperone pair previously reported (25), because the full-length recombinant YopE expressed by *E. coli* was not soluble. Our results suggest the possibility that YscM1 serves as an intermediate, promiscuous chaperone regulating the release and secretion of YopH and YopE effector proteins into host cells, previously hypothesized to occur sequentially (24). Hence, a hierarchical delivery of proteins through the injectosome may be partially controlled by the stability of chaperone-ligand complexes (Figure 4). In this model, stable complexes of YscM1-SycH are more numerous than YscM1-SycE complexes, in turn favoring transfer rates of YopH >YopE. An exchange of SycH with YscM1 drives YopH release into the mammalian host cell, and depletion of SycH-YopH complexes initiates the transfer of YopE by a similar mechanism. Further, our data indicate that SycE has a propensity to interact with YscM1 and the *Y. enterocolitica* protein YscM2, but not YopH. It is possible that YscM1, YscM2 and YopH may use similar binding modes due to a high degree of three-dimensional structural similarity among these SycH ligands (W. Swietnicki, unpublished results). However, YopE is the natural ligand of the SycE chaperone and *Y. pestis* and *Y. pseudotuberculosis* produce YscM1 (LcrQ) but not YscM2. This suggests that YscM2 retained affinity for SycE and SycH during evolution, perhaps serving a function redundant to YscM1.

References

1. Kubori, T., Matsushima, Y., Nakamura, D., Uralil, J., Lara-Tejero, M., Sukhan, A., Galan, J.E., and Aizawa, S.I. (1998). *Science* **280**, 602-605.
2. Cornelis, G.R. (2002). *J. Cell. Biol.* **158**, 401-408.
3. Neyt, C., and Cornelis, G.R. (1999). *Mol Microbiol.* **33**, 971-981.
4. Tardy, F., Homble, F., Neyt, C., Wattiez, R., Cornelis, G.R., Ruysschaert, J.M., and Cabiaux V. (1999). *EMBO J.* **18**, 6793-6799.
5. Andersson, K., Magnusson, K.E., Majeed, M., Stendahl, O., and Fallman, M. (1999). *Infect Immun*. **67**, 2567-2574.
6. Bliska, J.B., Guan, K.L., Dixon, J.E., and Falkow, S. (1991). *Proc. Natl. Acad. Sci. U.S.A.* **88**, 1187-1191.
7. Persson, C., Carballeira, N., Wolf-Watz, H., and Fallman, M. (1997). *EMBO J.* **16**, 2307-2318.
8. Andor, A., Trulzsch, K., Essler, M., Roggenkamp, A., Wiedemann A., Heesemann, J., and Aepfelbacher, M. (2001). *Cell. Microbiol.* **3**, 301-310.
9. Barz, C., Abahji, T.N., Trulzsch, K., and Heesemann, J. (2000). *FEBS Lett*. **482**, 139-143.
10. McDonald, C. Vacratsis, P.O., Bliska, J.B. and Dixon, J.E. (2003) *J. Biol. Chem*. **278**, 18514-23.
11. Neyt, C., and Cornelis, G.R. (1999). *Mol Microbiol.* **31**, 143-156.
12. Wattiau, P., Bernier, B., Deslee, P., Michiels, T., and Cornelis, G.R. (1994). *Proc. Natl. Acad. Sci. U.S.A.* **91**, 10493-10497.

13. Birtalan, S.C., Phillips, R.M., and Ghosh, P. (2002). *Mol Cell*. **9**, 971-980.

14. Cambronne, E.D. and Schneewind, O. (2002). *J Bacteriol*. **184**, 5880-5893.

15. Darwin, K.H., and Miller, V.L. (2001). *EMBO J.* **20**, 1850-1862.

16. Skurnik, M., and Toivanen, P. (1992). *J. Bacteriol.* **174**, 2047-2051.

17. Yother, J., Chamness, T.W., and Goguen, J.D. (1986). *J. Bacteriol.* **165**, 443-447.

18. Evdokimov, A.G., Tropea, J.E., Routzahn, K.M., and Waugh, D.S. (2002). *D Biol. Crystallogr.* **58**, 398-406.

19. Fox, J. D. and Waugh, D. S. (2003). *Methods Mol. Biol.* **205**, 99-117.

20. Evdokimov, A. G., Tropea, J. E., Routzahn, K. M., Copeland, T. D., and Waugh, D. S. (2001). *Acta Crystallogr. D Biol. Crystallogr.* **57**, 793-799.

21. Brandler, P., Saikh, K.U., Heath, D., Friedlander, A., and Ulrich, R.G. (1998). *J Immunol* **161**, 4195-4200.

22. Stebbins, C.E., and Galan, J.E. (2001). *Nature* **414**, 77-81.

23. Cambronne, E.D., Cheng, L.W., and Schneewind, O. (2000). *Mol. Microbiol.* **37**, 263-73.

24. Wulff-Strobel, C.R., Williams, A.W., and Straley SC. (2002). *Mol. Microbiol.* **43**, 411-423.

25. Cheng, L.W. and Schneewind, O. (1999). *J. Biol. Chem.* **274**, 22102-8.

26. Lawton, D.G., Longstaff, C., Wallace, B.A., Hill, J., Leary, S.E., Titball, R.W., and Brown, K.A. (2002). *J. Biol. Chem*. **277**, 38714-38722.

27. Fields, K.A., Nilles, M.L., Cowan, C., and Straley S.C. (1999). *Infect. Immun*. **67**, 5395-5408.

28. Francis, M.S., Aili, M., Wiklund, M.L., and Wolf-Watz, H. (2000). *Mol Microbiol*.

38, 85-102.

29. Francis, M.S., Lloyd, S.A., and Wolf-Watz, H. (2001). *Mol Microbiol*. **42**, 1075-1093.
30. Woestyn, S., Sory, M.P., Boland, A., Lequenne, O., and Cornelis, G.R. (1996). *Mol. Microbiol*. **20**, 1261-1271.
31. Birtalan, S. and Ghosh, P. (2001). *Nat. Struct. Biol*. **8**, 974-978.
32. Montagna, L.G., Ivanov, M. I., and Bliska, J. B. (2001). *J. Biol. Chem*. **276**, 5005-5011.
33. Iriarte, M., Sory, M.P., Boland, A., Boyd, A.P., Mills, S.D., Lambermont, I., and Cornelis, G.R.(1998). *EMBO J.* **17**, 1907-1918.
34. Madrid, C., Nieto, J.M., and Juarez, A. (2002). *Int. J. Med. Microbiol.* **291**, 425-432.
35. Nieto, J.M., Madrid, C., Miquelay, E., Parra, J.L., Rodriguez, S., and Juarez A. (2002). *J. Bacteriol*. **184**, 629-635.
36. Smith, C. L., Khandelwal, P., Keliikuli, K., Zuiderweg, E. R. P., and Saper, M. A. (2001). *Mol. Microbiol.* **42**, 967-979.
37. Francis, M.S. and Wolf-Watz, H.(1998). *Mol. Microbiol.* **29**, 799-813.
38. Skrzypek, E., Cowan, C., and Straley, S.C. (1998). *Mol. Microbiol*. **30**, 1051-1065.
39. Lee, V. T. and Schneewind, O. (1999). *Mol Microbiol*. **31**, 1619-1629.
40. Day, J.B., Guller, I., and Plano, G.V. (2000). *Infect. Immun*. **68**, 6466-6471.
41. Stainier, I., Iriarte, M., and Cornelis G.R. (1997). *Mol Microbiol.* **26**, 833-843.
42. Payne, P.L. and Straley, S.C. **(**1999). **181**, 2852-2862.
43. Stainier, I., Bleves, S., Josenhans, C., Karmani, L., Kerbourch, C., Lambermont, I.,

Totemeyer, S., Boyd, A., and Cornelis, G.R. (2000). *Mol Microbiol*. **37**, 1005-1018.

44. Du, Y., Rosqvist, R., and Forsberg, A. (2002). *Infect Immun*. **70**, 1453-1460.

45. Zav'yalov, V.P., Chernovskaya, T.V., Navolotskaya, E.V., Karlyshev, A.V., MacIntyre, S., Vasiliev, A.M., and Abramov, V.M. (1995). *FEBS Lett*. **371**, 65-68.

46. Lee, V.T., Anderson, D.W., and Schneewind, O. (1998). *Mol. Microbiol*. **28**, 593-601.

Figure Legends

Figure 1. Matrix of protein-protein interactions of *Y. pestis* TTSS based on surface plasmon resonance and mass spectrometry results. Each interaction pair was assigned a relative strength according to the instrument response: red – strong (>300 RU), green – medium (100-300 RU), yellow – weak (50-100 RU), and gray – background (0-50 RU). Interactions were measured at 37^{o} C in 10 mM potassium phosphate, pH = 7.0, 150 mM NaCl. Analyte concentration was 1 μM. Total protein density on the CM5 chip was 2000 - 4000 RU/flow cell. Proteins pairs found to form a complex by mass spectrometry were marked with a "+" sign, and those not confirmed by mass spectrometry were marked with "-." ND - not determined.

Figure 2. Interactions of TTSS components measured by surface plasmon resonance. Representative sensograms of select protein pairs exhibiting strong interactions: surface immobilized – analyte in solution.

Figure 3. Mass spectra of selected protein - protein complexes between components of the *Y. pestis* type III secretion system. Spectra are for interaction pairs scored as (A) – strong, (B) – medium, (C) – weak, and (D) – background based on the surface plasmon resonance measurements. Experimental masses are listed under each protein. Proteins were incubated at 37^{o} C in 10 mM potassium phosphate, pH = 7.0, 150 mM NaCl for 30 min. and then prepared for MALDI – TOF measurements as described under Materials and Methods. The protein concentration was 5 μM for each component.

Figure 4. Hypothetical hierarchical model of YopE and YopH injection

Assumptions: SycE, SycH and YscM1 all form stable homo-dimers.

[YscM1-SycH] > [YscM1-SycE]

SycE and SycH remain in bacterial cells (46).

Unknowns: Stable YopE-YscM1 complex.

Table I. Proteins used in this study

Protein	Sequence[a]	Function	Potential partner
LcrG	**G** - (1 - 95) – **HHHHHH**	Together with LcrV responsible for targeting of Yops[26, 27]	LcrV
LcrH	**G** – (1 - 168) - **HHHHHH**	Together with YopD involved in negative regulation of Yops synthesis[14, 28, 29]	YopD
SycE	(1 – 130)	Chaperone for YopE[13, 18, 30, 31]	YopE
SycH	(1 – 138)	Chaperone for YopH [22, 32]	YopH YscM1,YscM2
TyeA	**S – HHHHHH** – (2 – 92)	Involved in translocation of YopE and YopH[33]	YopD LcrE (YopN)
YmoA	**G** – (1 - 67) - **HHHHHH**	Thermal regulator of virulence factors expression[32, 33]	H-NS[c]
YopH/N	**M** - (2 - 129) - **HHHHHH**	Tyrosine phosphatase disrupts focal adhesions[32, 36]	SycH
YopH/C	**M** - (164 – 468)		

Table I. Continued.

Protein	Sequence[a]	Function	Potential partner
YopK	**G** - (1 - 182) - **HHHHHH**	Translocation apparatus[37]	Unknown
YopM[b]	**G** – (1 - 367) - **HHHHHH**	Effector protein of unknown function[10, 33, 38]	Unknown
YopR	**S - HHHHHH** - (2 -165)	Translocation apparatus[39]	Unknown
YscE	**S** – **HHHHHH** – (2 - 66)	Controls secretion of Yops[40]	YscG
YscM1[c]	**G** – (1 - 115) - **HHHHHH**	Negative regulator of Yops secretion[22, 41]	SycH
YscM1/N-term	**M** – (29-78) - **HHHHHH**		SycH
YscM2[d]	**S - HHHHHH** - (1 - 116)	Negative regulator of Yops secretion[14, 41]	SycH
YscP	**S – HHHHHH** – (1 – 455)	Controls secretion of Yops[42, 43]	Unknown
F1	(22-170)	Capsular antigen proposed to interact with cellular receptor[44, 45]	Unknown

[a]Bold characters mark the sequence added for cloning and purification purposes. Numbers in parenthesis indicate start and end of the cloned protein sequence.

[b]Cloned from *Y. enterocolitica*. Residues 1- 198 are 100 % identical, and overall sequence is 92 % identical to the amino acid sequence of *Y. pestis* YopM.

[c]The YscM1 sequence used in this study is identical to the YscM1 sequence from *Y. enterocolica* and LcrQ from *Y. pestis*.

[d]The YscM2 sequence from *Y. enterocolica* is 59.1% identical (110 out of 116 total a. a.) to *Y. pestis* LcrQ. *Y. pestis* does not express YscM2.

Table II. Protein-protein interactions of the *Y. pestis* TTSS measured by MALDI-TOF[a]

Protein pair	M mass, exp. *Da*	MW, calc. *Da*	Complex formation	Molecular mass of complex, *Da*	
				Experimental	Calculated
YmoA YopK	8955 21811	8943.2 21879.6	yes	30666	30822.8
YmoA TyeA	8825 11534	8943.2 11531.9	yes	20290	20475.9
YmoA SycH	8818 15419	8943.2 15437.5	no	N/A	N/A
YopK SycH	21812 15536	21879.6 15437.5	yes	37368	37317.1
YopK LcrG	21816 11946	21879.6 11899.5	no	N/A	N/A
YscE SycE	8401 14632	8345.5 14649.6	yes	22973	23034.9
YscE LcrH	8500 19933	8345.5 19894.4	yes	28194	28278.9
YscE YmoA	8500 8955	8345.5 8943.2	yes	17617	17327.7
YscE TyeA	8500 11635	8384.5 11531.9	no	N/A	N/A
YscM1/N-term YopH/N-term	6427 14752	6536.3 14772.5	yes	21115	21308.8

Table II. Continued.

Protein pair	M Mass, exp. *Da*	MW, calc. *Da*	Complex formation	Molecular mass of complex, *Da*	
				Experimental	Calculated
YscM1/N-term SycH	6428 15410	6536.3 15437.5	yes	21779	21973.8
YscM1/N-term SycE	6416 14659	6536.3 14649.6	yes	21050	21095.9
YscM2 SycH	13649 15485	13757.8 15437.5	yes	28994[c]	29195.3
YscM2 TyeA	13654 11536	13757.8 11531.9	yes	25114	25353.9
YscM2 YopK	13800 21811	13757.8 21879.6	yes	35408	35637.1
YscM2 LcrH	13649 19864	13757.8 19894.4	yes	33425	33652.2
YscM2 SycE	13649 14719	13757.8 14649.6	yes	28005	28407.4
YscM2 YopH/N-term	13655 14754	13757.8 14772.5	yes	28336	28530.3
YscM2 YscE	13667 8395	13757.8 8345.5	no	N/A	N/A
YopH/N-term. TyeA	14760 11554	14772.5 11531.9	yes	26231	26314.4
YopH/N-term YopK	14758 21822	14772.5 21879.6	yes	36581	36652.1
YopH/N-term SycH	14766 15485	14772.5 15437.5	yes	30091	30210.0
YopH/N-term F1	14776 15528	14772.5 15648.3[b]	yes	30245	30420.8

Table II. Continued

Protein pair	M mass, exp. *Da*	MW, calc. *Da*	Complex formation	Molecular mass of complex, *Da*	
				Experimental	Calculated
F1	15542	15648.3[b]	no	N/A	N/A
LcrG	11974	11899.5			
TyeA	11548	11531.9	yes	33269	33411.5
YopK	21813	21879.6			
TyeA	11531	11531.9	yes	31307	31426.3
LcrH	19849	19894.4			

[a]Protein solutions at 5 μM total concentration of each component were incubated for 30 min at 37°C in 10 mM potassium phosphate buffer, pH=7.0, 150 mM NaCl, and then prepared for MALDI-TOF analysis as described under Materials and Methods. Complex formation for pairs involving YopH/C protein was not determined by MALDI-TOF due to strong tendency of the protein to precipitate under experimental conditions.

[b]The mass of recombinant F1 antigen was determined with ProtParam[47] from the sequence of the mature form of protein.

[c]A 2:1 stoichiometric complex of SycH-YscM2 was also detected.

Table III. Kinetic analysis of select TTSS interacting protein pairs.

Protein pair[a]	K_d[b]	k_a*10^3	k_d*10^{-3}	*Stable SEC complex*[c]
	μM	1/Ms	1/s	
LcrH-YscE	1.23 ± 0.01	4.56 ± 0.01	5.62 ± 0.01	no
YmoA-YscE	0.392 ± 0.01	9.39 ± 0.31	3.68 ± 0.07	no
TyeA-YscE	>5.0[d]			no
YscM1-SycE	1.9[d]			yes
YscM2-SycE	1.16 ± 0.01	9.8 ± 0.01	11.4 ± 0.04	yes
YopH/N-SycH	1.04 ± 0.02	1.39 ± 0.01	1.44 ± 0.03	yes
YscM1-SycH	0.053 ± 0.01	19.3 ± 0.15	1.02 ± 0.01	yes
YscM2-SycH	0.80 ± 0.01	0.84 ± 0.01	0.67 ± 0.01	yes

[a]Analysis by surface plasmon resonance. Immobilized to biosensor surface- in solution (analyte).

[b]K_d values were calculated as ratios of k_a/k_d determined from kinetics experiments.

Errors are reported for single experiments. Each experiment included duplicates of each solute concentration.

[c]Size exclusion chromatography (SEC)

[d]The value was estimated from saturation response data due to the rapid on/off-rates.

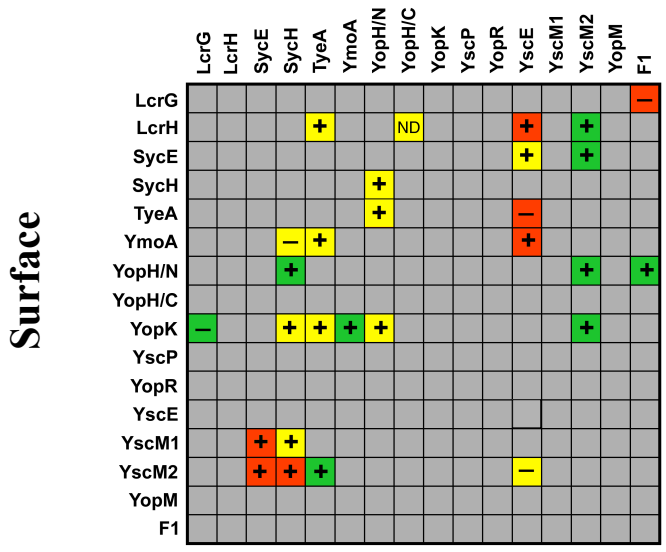
Analyte
Surface
LcrG
LcrH
SycE
SycH
TyeA
YmoA
YopH/N
YopH/C
YopK
YscP
YopR
YscE
YscM1
YscM2
YopM
F1
ND

Figure 1

A

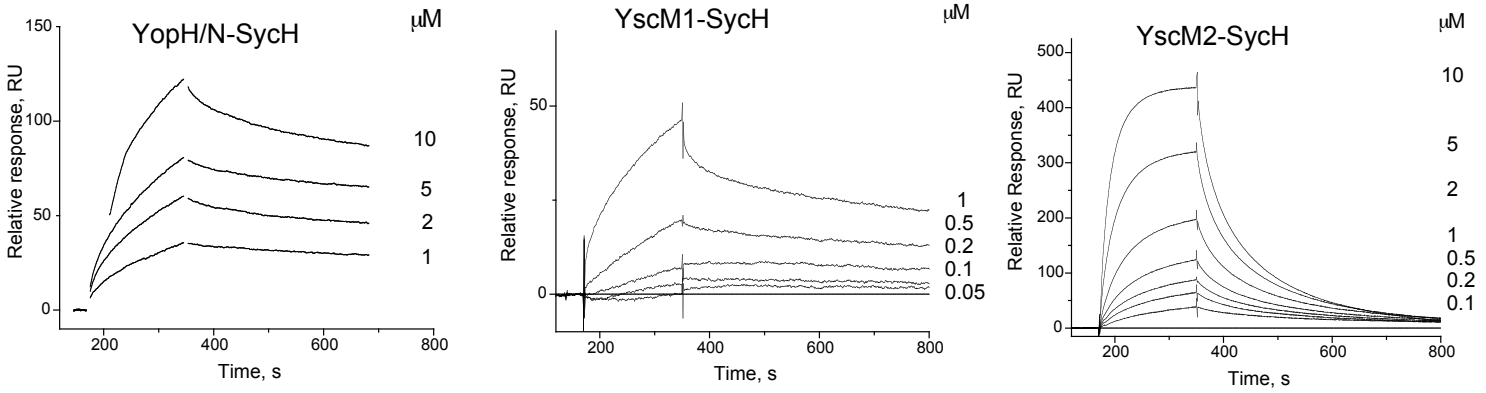
YopH/N-SycH
μM
10
5
2
1
Relative response, RU
Time, s
YscM1-SycH
μM
1
0.5
0.2
0.1
0.05
Relative response, RU
Time, s
YscM2-SycH
μM
10
5
2
1
0.5
0.2
0.1
Relative Response, RU
Time, s

B

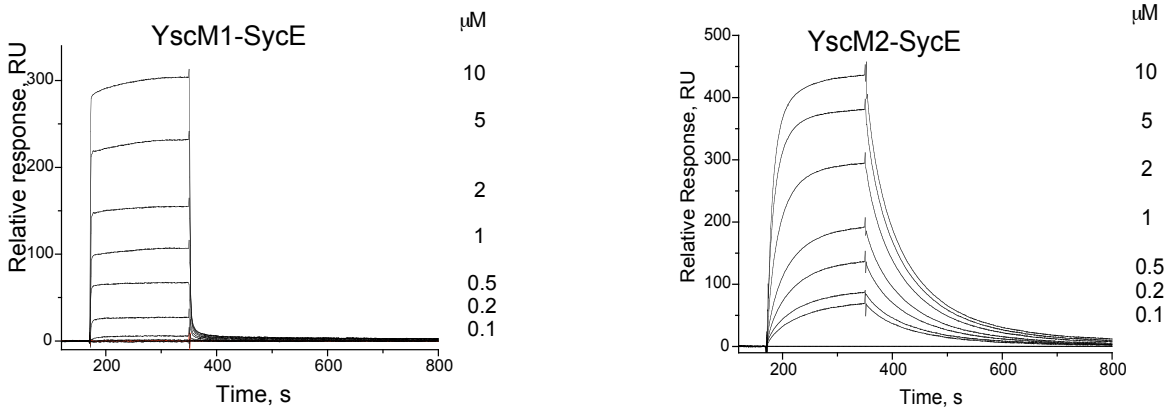
YscM1-SycE
μM
10
5
2
1
0.5
0.2
0.1
Relative response, RU
Time, s
YscM2-SycE
μM
10
5
2
1
0.5
0.2
0.1
Relative Response, RU
Time, s

C

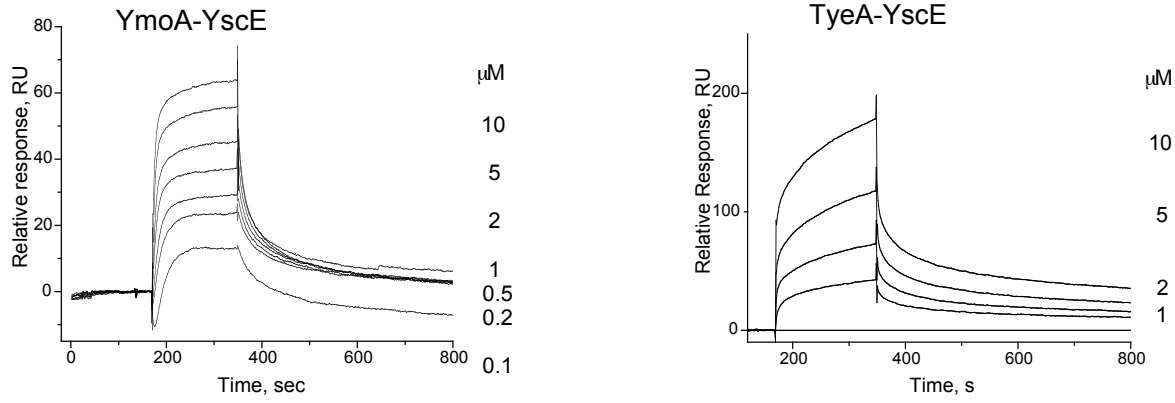
YmoA-YscE
μM
10
5
2
1
0.5
0.2
0.1
Relative response, RU
Time, sec
TyeA-YscE
μM
10
5
2
1
Relative Response, RU
Time, s

Figure 2

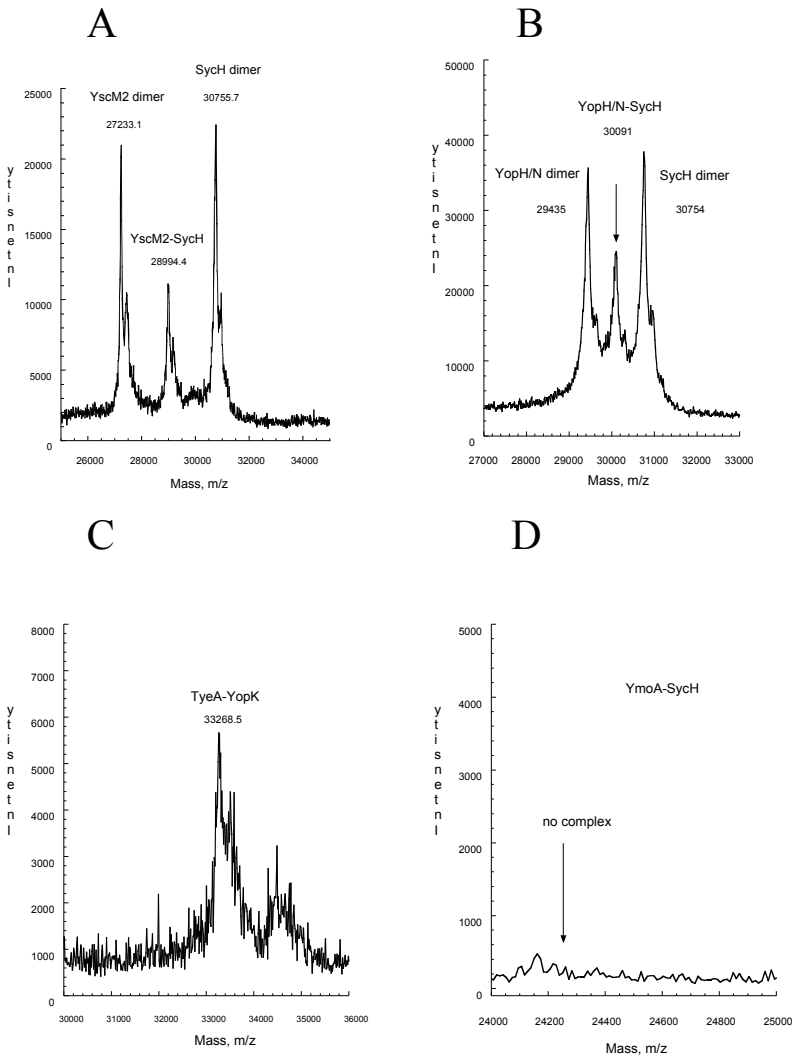
A
SycH dimer
YscM2 dimer
30755.7
27233.1
YscM2-SycH
28994.4
Intensity
Mass, m/z
B
YopH/N-SycH
30091
YopH/N dimer
29435
SycH dimer
30754
Intensity
Mass, m/z
C
TyeA-YopK
33268.5
Intensity
Mass, m/z
D
YmoA-SycH
no complex
Intensity
Mass, m/z

Figure 3

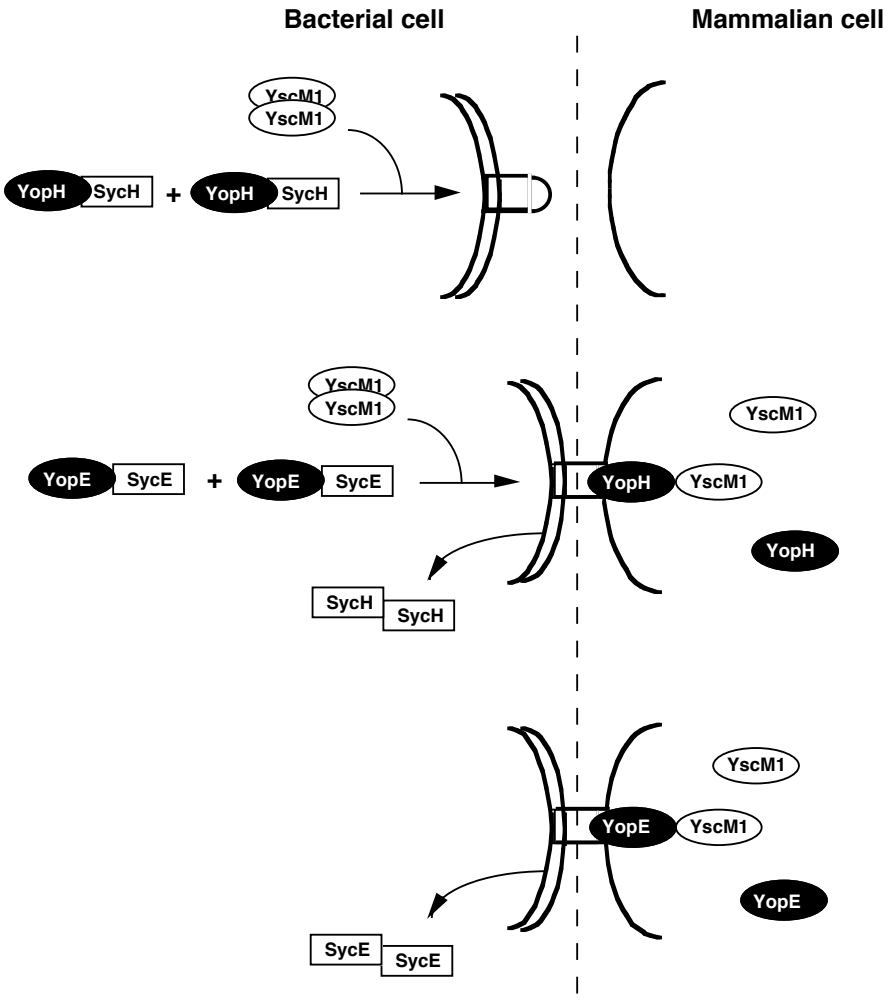
Bacterial cell
Mammalian cell
YscM1
YscM1
YopH
SycH
+
YopH
SycH
YscM1
YscM1
YopE
SycE
+
YopE
SycE
YscM1
YopH
YscM1
YopH
SycH
SycH
YscM1
YopE
YscM1
YopE
SycE
SycE

Figure 4.